The 2017 World Congress on
Advances in Structural Engineering and Mechanics (ASEM17)
Ilsan(Seoul), Korea, August 28 - September 1, 2017

Keynote Paper

A Unified Practical Approach for Estimating the Effects of Rare Dynamic Loading on Structures

Nelson Lam[1)]

Department of Infrastructure Engineering, the University of Melbourne, Parkville 3010, Australia
ntkl@unimelb.edu.au

ABSTRACT

Rare dynamic loading on a structure can be caused by an earthquake, impact by a vehicle or fallen boulder, accidental dropping of a heavy object or blast pressure generated by an explosion. Codes of practices for designing for seismic actions have been put in place for the calculation of the inertia forces generated by earthquake ground shaking. However, few guidelines are available for designing for other types of transient and dynamic actions. Engineers would often be required to rely on computer simulations employing specialist software to inform decision making in design. Difficulties in checking the computations and in verifying the simulated results are cause for concern. This paper presents overarching fundamental principles governing the behaviour of different forms of dynamic actions. Analytical techniques that have been extended for solving wider forms of transient Loading will also be presented**.**

1. INTRODUCTION

This paper was written in support of the keynote presentation that was delivered on the 30th of August 2017 to the ASEM17 symposium held in South Korea. No prior knowledge on extreme loading and on structural dynamics is required of the readers of this review article which is mainly concerned with impact actions. The author is also fortunate to have received support from a group of fellow academics and industry representatives in co-hosting a mini-symposium entitled "Code developments in regions of low to moderate seismicity". Those who have come across the idea of the use of a response spectrum to represent seismic actions, and have read the paper entitled " earthquake loading characterisation for regions of low to moderate seismicity " that was presented in the mini-symposium (Tsang & Lam 2017), should be able to draw the analogy between methods for dealing with seismic and non-seismic actions.

[1)] Professor

The concept of velocity controlled seismic actions which is represented by the "hyperbolic" part of the response spectrum for earthquake loads enlightens structural design engineers as to how kinetic energy is converted into elastic strain energy in the course of the response of the structure to a transient action (which is proportional to the product of force and displacement demand). The "hyperbolic" phenomenon is simply a manifestation of the trading- off of displacement demand with force demand in velocity controlled conditions. This idea is in analogy to how impulsive action of impact is analysed (which is the subject matter of this paper). The approach of equating momentum and energy has been around for a long time (refer literature review in Sec 2). Even then, many closed form expressions presented in this article have only been derived, and experimentally verified, very recently for accurate predictions of the destabilising action of the impact (sec. 3) and predictions of the deformation of a RC member (sec. 4). Interestingly, impact actions in the elastic range may be represented by a response spectrum like seismic actions when linear elastic behaviour of the affected structure can be assumed. The same can be said of blast actions which is also transient in nature although it is outside the scope of the paper. The models that have been developed is versatile enough for adaptation to non-linear (post-elastic) behaviour of the member. Applying the unified concept of equating energy and momentum across different types of load scenarios is the main thrust of the paper.

The localised action of the contact force of impact as introduced in the later part of the article is unique to the impact action of a solid object given that no such contact force is generated by an earthquake. Although contact force is complex to model because of its non-linear nature a simple numerical algorithm has been developed and experimentally verified for predicting the forcing function (sec. 5). The benefits of identifying the forcing function is in emulating an impact action by the use of an actuator thereby cutting down on the cost of physical experimentation. Furthermore, a quasi-static test has the advantage over impact test in that the ultimate capacity of the target can also be found.

2. STATE-OF-THE-ART REVIEW

2.1 Impact Action on Reinforced Concrete

Research that has been undertaken on the impact-resistant behaviour of reinforced concrete was mostly experimental in nature (e.g. Mougin 2005; Kishi and Mikami, 2012; Wu, 2015). Experiments that have been conducted typically feature applying the impact of a drop weight from varying heights. Much of those drop tests on RC beams were aimed at determining the manner in which the impact resistant behaviour of RC can be controlled by reinforcement design and detailing. RC slabs that were built of concrete of different mixes and different types of reinforcing have also been tested. For example, a drop weight of 183 kg was made to impact on a RC slab specimen of dimensions: 3.35 m x 1.52 m x 0.09 m in Zineddin & Kranthhammer (2007) and another specimen of a thicker slab of dimension 1 m x 1 m x 0.15 m in Hummelternberg (2011). Many of these investigations were *adhoc* in nature. Thus, a holistic set of design guidelines (in RC design and detailing) for countering impact

actions could not be derived from the reported findings. Empirical closed-form expressions have also been derived from regression analysis of experimental results reported in Zhan (2015). However, data that have been obtained for use in regression analysis were specific to impact scenarios employed in the testing and hence the algebraic expressions so derived lack generality. With certain impact experiments time-histories of acceleration and/or displacement were recorded as reported in Fujikake (2009); Chen & May (2009) and Kishi & Bhatti (2010). These recorded forcing functions and response time-histories can be used potentially for the verification of results from computer simulations based on finite element modelling (FEM).

Software packages namely that of LS-DYNA and ABAQUS for FEM are also used frequently for simulating impact actions and the behaviour of the structure responding to the impact (Kishi 2009; Yang 2012a & 2012b; Berthet-Rambaud 2003; Thai 2014; Chikatamaria 2004; Delhomme 2007; Kishi & Bhatti 2010). Computer simulations employing FEM or Discrete Element Modelling (DEM) have been proven to be a powerful technique to simulate impact scenarios that closely resemble real conditions. Once the calibrated model has been verified experimentally, FEM (which can be used in conjunction with DEM) can be employed for studying the effects of the change in the geometry and dimensions of the target. However, an important limitation of computer modelling is that certain input parameters into the model can be ambiguous. For example, material models and their characterising parameters need to be carefully chosen from the list of pre-defined constitutive models that have been built into the software for both the impactor object and the target. LS-DYNA provides more than 250 choices of materials to the users (LS-DYNA 2015). Concrete alone has at least eight different constitutive models to choose from. Thus, it can be difficult to decide which particular material model to give satisfactory results even though results of comparisons between the models are available to the users (e.g. Wu 2012).

2.2 Impact Action on a Vehicular Barrier

The impact action of a vehicle on a bridge pier, or vehicular parapet, on a highway is represented by a prescribed equivalent static load. In AS5100.2 (SA 2004), for example, the stipulated design collision force from road traffic on a bridge support is 2000 kN which is applied at 10 degrees from the direction of the road alignment. Similar format of design load stipulations for structures that are vulnerable to collision on a highway have been adopted by major codes of practices in other parts of the world including United Kingdom, Japan, Australia, Germany and the United States (BSI 2008; JRA ; Standards Australia 2004, ASTRA 2008, AASHTO 2012; Austroads 2013). This simple format of quantifying impact action as an equivalent static force is convenient for structural design purposes. However, the actual amount of force generated by an impact cannot be determined by considering the vehicle alone as it is also dependant on the interaction with the pier (or barrier). The limitations of the equivalent static force provision has not been well explained in structural design codes of practices. Consequently, the extent in which existing equivalent static force provisions can be adapted for the design and analysis of a diversity of impact scenarios remains uncertain.

The alternative equal energy method has a theoretical basis which is easy to explain and appears to be versatile. For example, expressions of the form of Eqs.(1a) – (1c) as presented in *Annex C* of Eurocode 1 (BSI 2008) for horizontal "hard impact" scenarios are based on *equal energy principles*.

$$\frac{1}{2}mv_0^2 = \frac{1}{2}k\Delta^2 \tag{1a}$$

$$\Delta = \frac{mv_0}{\sqrt{km}} \tag{1b}$$

$$F = k\Delta = v_0\sqrt{km} \tag{1c}$$

where m is mass of *impactor*, v_0 is the cruising velocity, k is the stiffness of the linear elastic system, Δ is the impact induced deflection of the target and F is the equivalent static force to match with the displacement demand.

Contemporary codes of practices for the design of vehicular barriers represented by Eqs.(1a) – (1c) were derived from the principles of equating kinetic energy of the moving vehicle with the energy absorbed by the deforming target (the barrier). A similar method of calculation has been used to predict the maximum force imposed by a crumbling vehicle onto a rigid concrete profiled barrier in which case the initial kinetic energy is assumed to be dissipated wholly with the vehicle. With both examples, the energy absorption is assumed to be wholly taken up by only one element of the impact (i.e. the impactor or target).

2.3 Impact Action of a Fallen Object

To analyse scenarios featuring the dropping of an *impactor* of mass (m) from height (h), the *left-hand-side* of the *equal energy* equation Eq. (2a) requires a term representing the loss of potential energy of the *impactor*, $mg(h+\Delta)$. The term on the right hand side of the equation represents the elastic strain energy of absorption. Eq. (2) is an explicit function for finding the displacement demand (Δ) of the impact assuming linear elastic behaviour.

$$\Delta = \Delta_s\left\{1+\sqrt{1+\frac{2h}{\Delta_s}}\right\} \quad \text{where} \quad \Delta_s = \frac{mg}{k} \tag{2}$$

where Δ_S is static displacement, h is drop height and k is member stiffness

Eqs. (1) – (2) are well known and easy to use provided that both the *impactor* and the structural system (target) can be idealised into respective connected lumped masses. However, the limitations of these expressions are not well understood. Clearly, the dissipation of energy occurring on impact has not been taken into account. Contributions by the inertial resistance of the target is also not taken into account given that the target mass has not been included as a parameter in the expressions. Thus, little is known of how much error is incurred by the use of these equations. These uncertainties coupled with the absence of evidences from physical experimentations for

supporting the use of the expressions have resulted in their limited use in practice.

2.4 Impact Action on Building Facades

The failure of corrugated panels, and composite insulated panels, against windborne debris impact have also been studied (Fernandez 2010; Chen 2014; Herbin & Barbato 2012).Sophisticated finite element software packages such as LS DYNA, ABAQUS, and ANSYS have been employed in the literature (Chen 2014; Herbin & Barbato 2012; Yahya 2012; Goyal 2013; Raguraman 2008) to simulate damage by impact actions to circumvent the need of costly impact experimentation. However, the ability of the model to accurately simulate impact scenarios is often uncertain. Much of the uncertainties are related to parameter values for input into the impact analysis for characterising the dynamic properties of the impactor and the target. Impact fragility curves for storm panels have also been developed by the use of experiments and stochastic finite element models (Herbin & Barbato 2012; Alphonso & Barbato 2014) to study the effects on building facades of debris impact. In summary, research into impact by windborne debris as reported in the literature (Fernandez 2010; Chen 2014; Zhou 2014; Frye 2012; Chen & Hao 2015) is mostly about observing, and simulating damage to specific types of targets as opposed to quantifying the impact action for a given impact scenario.

2.5 Localised Action of Impact

An impact action can be resolved into the global deflection demand of the impact and localised contact force. The global deflection demand resulted from the impact can be estimated by equating momentum and energy as described above and can be emulated by what is known as an equivalent static force. The value of quasi-static force F_{qs} can be estimated by taking the product of the stiffness of the target (k) and its maximum deflection resulted from the impact action (Δ). The value of F_{qs} should also be equal to the difference between the contact force and the maximum inertia force. Thus, F_{qs} has also referred as the *reaction force*.

Impact force may also refer to the *Peak Contact force* which is experienced by the surface of the target at the point of contact with a hard impactor object. Contact force is is much higher than the equivalent static force because of interferences from inertia forces generated within the target, and lasts for only a few milliseconds whereas the deflection of the target evolves over a much longer period depending on the natural period of vibration of the targeted element. In summary, "Impact force" is a general term which can carry different meanings as it may refer to the *quasi-static force* which is the force applied to the target to result in the same amount of maximum deflection generated by the impact action (and not to be confused with the force at contact controlling the amount of indentation into the metal cladding).

A simple, and common, way of estimating contact force generated at the point of contact between a spherical object and the surface of the target is based on the use of the non-linear contact force model which defines the relationship between force and indentation into the surface of the target which is assumed to be made of a

homogeneous material possessing elastic properties. The value of the contact force is obtained by equating the kinetic energy delivered by the impact with the elastic strain energy. The mass and velocity of the impactor, its elastic modulus, and its radius at the position of contact (taking an equivalent spherical object to represent the impactor) are parameters characterising the impact action. The elastic modulus of the surface material which is subjected to the impact is the parameter characterising the potential compressive behaviour of the target when impacted upon.

The *contact force – displacement* ($F_c - \delta$) relationship can be expressed in the following form which is referred herein as the *Hertz* equation:

$$F_c = k\delta^p \tag{3a}$$

where displacement (δ) is defined as the amount of movement of the centre of the impactor object resulted from both the "squashing" of the object and "indentation" into the surface of the target; and k and p are coefficients for characterising the compressive behaviour of the impactor object and the surface of the target.

This $F_c - \delta$ behaviour can be used to characterise the behaviour of the *frontal* spring in the two-degree-of-freedom (2DOF) spring connected lumped mass system and is not to be confused with the behaviour of the *rear* spring which is in support of the target lumped mass. Once the values of k and p are known the maximum value of the displacement (δ) can be estimated using the following equation which is expressed in terms of the basic impact parameters (impactor's mass m and impacting velocity v_0):

$$\frac{1}{2}mv_0^2 = \int_0^{\delta_0} F_c \, d\delta = \int_0^{\delta_0} k\delta^p \, d\delta = \frac{k}{p+1}\delta_0^{p+1} \tag{3b}$$

$$\delta = \left(\frac{p+1}{2k}mv_0^2\right)^{\frac{1}{p+1}} \tag{3c}$$

Eqs. (3b) – (3c) are based on the assumption that no energy is dissipated in the loading phase of the impact (when the impactor is compressed). Mitigating effects which are derived from interactions between the impactor and the target have also been ignored. In spite of these assumptions, reasonable results can be obtained from these equations in a typical scenario where the duration of contact is an order of magnitude shorter than the time taken by the target to displace. The value of F_c is accordingly defined by the following expression based on substituting Equation (3c) into Equation (3a) as explained in Sun (2015a):

$$F_c = k\left(\frac{p+1}{2k} m v_0^2\right)^{\frac{p}{p+1}} \quad (3d)$$

The value of the exponent *p* is often taken the value of 1.5 by default as per Hertz Law. If the value of the material constants namely the Young's Modulus (*E*) and Poisson's ratio (ν) are known then the following expressions which are well established in the field of contact mechanics may be used for estimating the value of k.

$$p = 1.5 \quad (3e)$$

$$k = \frac{4}{3} E\sqrt{R} \quad (3f)$$

$$\frac{1}{E} = \frac{1-\nu_1^2}{E_1} + \frac{1-\nu_2^2}{E_2} \quad (3g)$$

$$\frac{1}{R} = \frac{1}{R_1} + \frac{1}{R_2} \quad (3h)$$

where $E_1$and ν_1 and E_2 and ν_2 are the *Young's* Modulus and *Poisson's* ratio of the impactor and target material respectively; and R_1 and R_2 are their respective radius of curvature (i.e. $1/R_2 = 0$ if surface of the target is flat).

There are limitations of model involving the use of the *Hertz* equation. The following assumptions have to be made:

I. The contact surfaces are continuous and non-conforming.
II. The material is homogeneous and the strains are small and within the elastic limit (this assumption of homogeneity, and the adoption of linear elastic material properties, means that the model is only valid if a spherical impactor object is not compressed by more than 10% of its diameter).
III. Each body is considered an elastic half-space, i.e. the contact area is much smaller than the characteristic dimensions of the contacting bodies.
IV. The contact surfaces are frictionless.
V. Energy dissipation in the course of the load application can be neglected (this assumption can result in overly conservative predictions of the peak contact force).

3. MODELLING THE DESTABILISING EFFECTS OF AN IMPACT

Consider a concrete barrier of rectangular cross-section. The barrier is subject to the impact of a flying object of mass (m) striking the top of the barrier, of height (*h*), at an incident velocity (v_o^2); refer Fig. 1. The amount of kinetic energy transferred to the barrier of rectangular section and of mass (M) can be turned into potential energy as the barrier undergoes rotation. This energy transfer is associated with the lifting of the centre of gravity by a vertical displacement $\Delta_{\text{C.G.}}$.

Eq. (4a) was derived and verified experimentally in Lam (2017) for the finding the value of $\Delta_{\text{C.G.}}$. The gain in potential energy of the barrier that has been lifted is represented by the left hand side of Eq. (4a) whereas the fraction of kinetic energy expanded on the lifting is represented by the right hand side of the expression. Given the value of $\Delta_{\text{C.G.}}$ the amount of rotation of the barrier, θ, can be found using Eq. (4c).

$$Mg\Delta_{\text{C.G.}} = \frac{\kappa h}{R}\left(\frac{1+\text{COR}}{1+\kappa}\right)^2\left(\frac{1}{2}mv_0^2\right) \tag{4a}$$

$$\kappa = \frac{I_\theta}{mhR} \tag{4b}$$

$$\theta = \sin^{-1}\left(\frac{\frac{h}{2}+\Delta_{\text{C.G.}}}{r}\right) - \beta \tag{4c}$$

where $r = 0.5\sqrt{h^2+w^2}$ and $\beta = \tan^{-1}\left(\frac{h}{w}\right)$.

I_θ is the rotational inertia of the rectangular barrier

and dimensions r (and $R = 2r$), w and h are as defined in Fig. 1.

The factor of safety (FOS) against overturning for a projected impact scenario is defined herein as $\Delta_{\text{C.G.(crit)}}/\Delta_{\text{C.G.}}$. It follows that FOS is a function of $\Delta_{\text{C.G.}}$, h and w. A design chart based on the use of dimensionless ratios $\Delta_{\text{C.G.}}/w$ and h/w, is shown in **Fig.** 2. The chart covers aspect ratios (h/w) up to 10 and curves corresponding to a range of FOS from 1 to 5 are shown.

In summary, the stability of a free-standing rectangular barrier against overturning can be assessed in four simple steps:

I. Calculate $\Delta_{\text{C.G.}}$ using Eq. (4a).
II. Calculate ratios $\Delta_{\text{C.G.}}/w$ and h/w.
III. Use of design chart of Fig.2 to identify the FOS against overturing

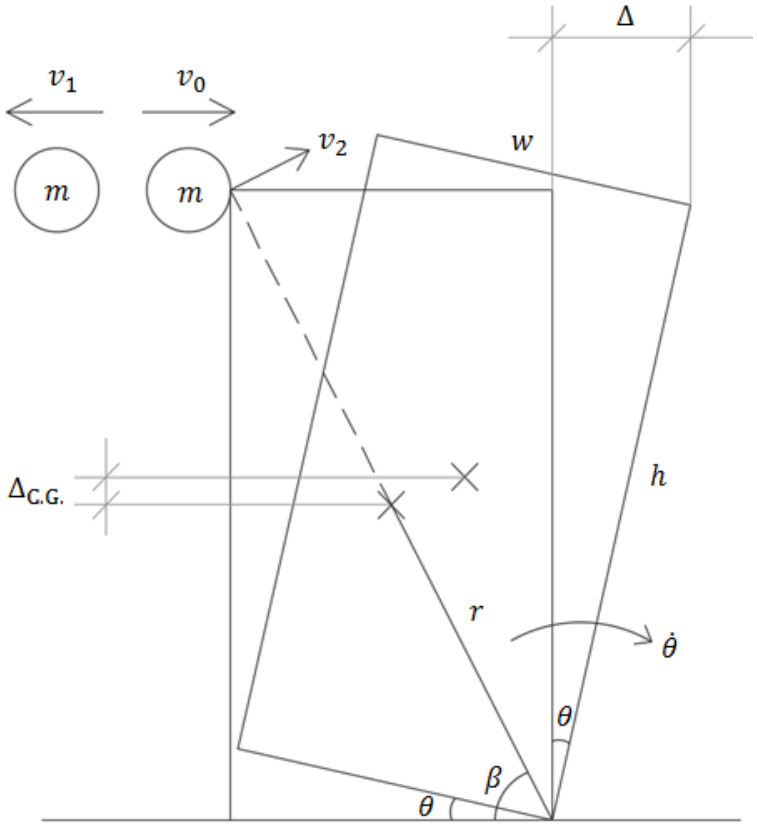

Fig. 1 Rectangular rigid barrier experiencing rocking effect under boulder impact

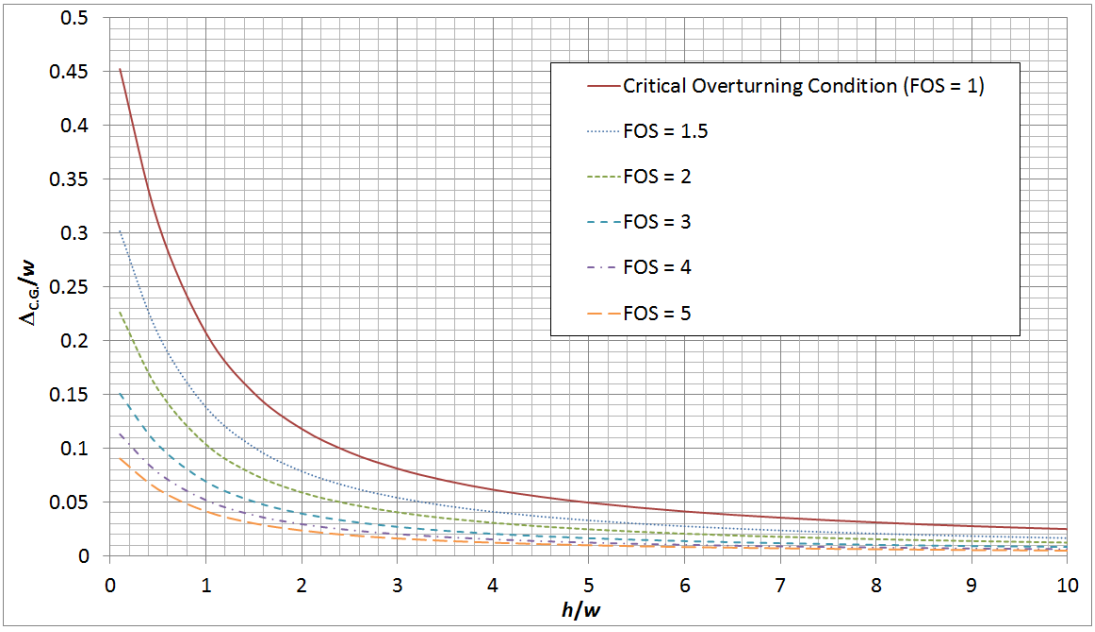

Fig. 2 Design chart for finding factor of safety from overturning

4. MODELLING THE BENDING ACTION OF AN IMPACT

The use of a quasi-static force to emulate impact conditions is based on deflecting the (RC) member by an amount equal to that predicted for a given impact scenario. To give such predictions momentum and energy principles are typically applied to a spring connected lumped mass analytical model (Fig. 3) which is a simplified representation of the targeted structural element (Yang 2012a). The value of the generalised mass (αm) and stiffness (k) assumed for the target is dependent on the boundary conditions of the element (refer Fig. 4). Similar recommendations for plate elements can be found in the literature (Yang 2012b).

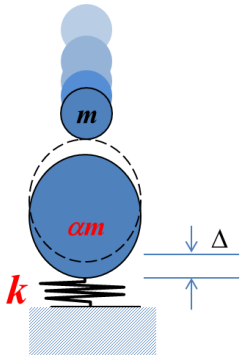

Fig. 3 Spring-connected lumped mass model

The amount of deflection (Δ) sustained by the target lumped mass in an impact scenario can be found by simply equating the kinetic energy delivered by the impactor with the energy of absorption as defined by Eqs. (5a) & (5b). The amount of deflection is accordingly given by Eq. (5c) which need to have also taken into account energy losses occurring in the course of the impact. Such energy losses can be parameterized in the form of *coefficient of restitution* (COR); refer Eqs. (5d) & (5e). Finally, the amount of quasi-static force to emulate the impact generated deflection is given by Eq.(5f). Should the displacement surpass the point of yielding Eq. (5g) may be used for predicting the total displacement which is the sum of the displacement at yield and the post-elastic displacement.

Importantly, experimental verifications of the proposed relationships can be found in Ali (2014). Expressions that have been presented in the above for analysing the impact action of a solid object can be represented in the form of an *acceleration-displacement response spectrum* (ADRS) diagram of Fig. 6a which is shown alongside the ADRS diagram for seismic actions (6b). The use of the latter diagram has been illustrated in the *Commentary* to the *Australia Standard for Seismic Actions* (AEES 2009).

The use of Eqs. (5a) – (5g) for analysing the impact action of a flying object is illustrated in the following example of a steel pole which is struck by the flying object at the top. It is required to calculate the maximum horizontal deflection of the pole in order that the amount of *quasi-static* force (F_{qs}) representing the impact can be found. Once the value of F_{qs} is known the bending moment and shear force at the base of the pole can be calculated accordingly.

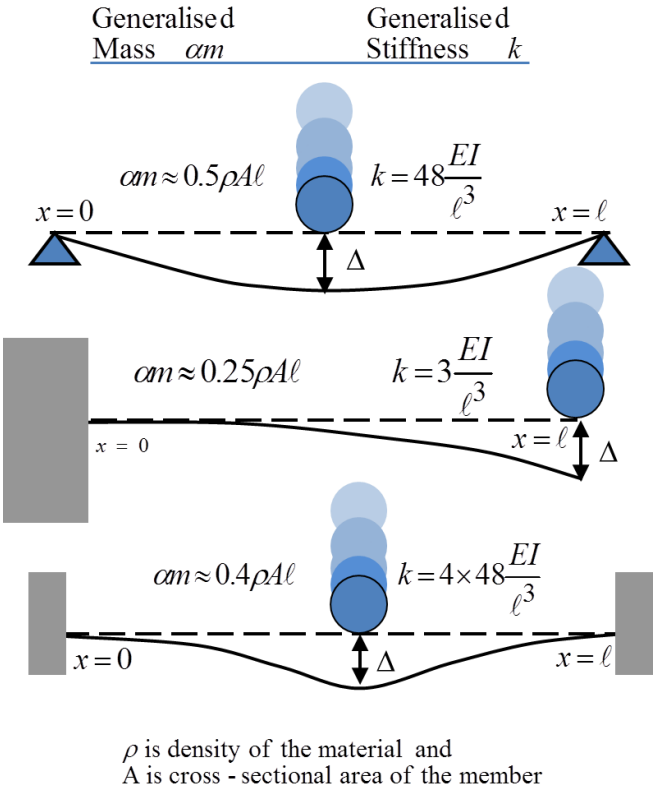

Fig. 4 Generalised mass and stiffness of structural elements

Equating momentum :

$$mv_o = -mv_1 + \lambda mv_2 \qquad (5a)$$

where m is mass of impactor and velocities v_o v_1 and v_2 are as defined in Fig.5

Equating the fraction of kinetic energy transferred to the member with the elastic strain energy of absorption :

$$\frac{1}{2}mv_o^2\beta^2 = \frac{1}{2}k\Delta_o^2 \qquad (5b)$$

$$\Delta = \frac{mv_o}{\sqrt{mk}}\beta \qquad (5c)$$

where

$$\beta = \sqrt{\lambda\left(\frac{1+\mathrm{COR}}{1+\lambda}\right)^2} \qquad (5d)$$

$$COR = \frac{v_1 + v_2}{v_o} \qquad (5e)$$

The quasi - static force F_{qs} is accordingly given by

$$F_{qs} = k\Delta = v_o\sqrt{mk}\beta \qquad (5f)$$

$$\Delta = \frac{mv_0^2}{2F_y(1+\lambda)} + \frac{\Delta_y}{2}$$ where Δ_y is deflection at yield (5g)

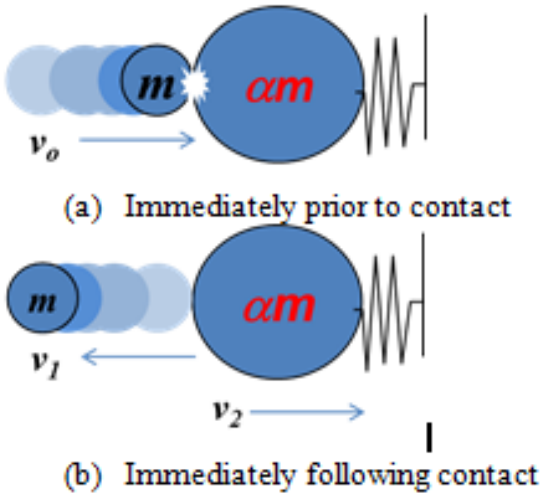

Fig. 5 Basis of equating momentum

In this example, the flying object weighs **40** kg and impact at the upper end of the steel pole at an incident velocity of **30** m/s. The 3m tall steel pole has flexural rigidity (*EI*) of **9 x 10^4** kNm^2 and is fixed at its base. The spring stiffness (k) of the spring connected lumped mass model is estimated to be 10^4 kN/m (being $3EI/h^3$). The self-weight of the steel pole is **960** kg per m length which is translated to a total mass of 2880 kg and a target mass (λm) in the lumped mass model of 720 kg (being ¼ of the total mass). The mass ratio λ is accordingly equal to 18 (being 720/40). The impactor is assumed to rebound with a *Coefficient Of Restitution* of 0.2. Linear elastic behaviour of the steel pole may be assumed.The horizontal deflection of the pole (Δ) and the corresponding quasi-static force (F_{qs}) can be found by substituting the values of various impact parameters into Eqs. (5c) and (5f) as shown by the following calculations:

$$\Delta = \frac{40\times 30}{\sqrt{40\times 10^7}}\sqrt{18\times\left(\frac{1+0.2}{1+18}\right)^2} = 0.016\,\text{m} \quad (6a)$$

$$F_{qs}(\text{kN}) = k\Delta = 10^4\times 0.016 = 160\text{kN} \quad (6b)$$

The *shear force* and *bending moment* at the base of the pole is accordingly 160 kN and 480 kNm respectively. The calculations have been repeated for poles of the same cross-section but with height varying between 0.5 m and 5 m to track the trend of change in the bending moment demand at the base. Results of calculations as shown in *Fig.* demonstrates the interesting phenomenon of significant decrease in the bending moment value with increasing height of the pole which is contrary to predictions by the conventional approach (based on the notion of representing the impact by a prescribed equivalent horizontal force).

Clearly, the impact hazard can be overstated significantly by simply representing the impact action by an equivalent force without allowing for contributions by the inertial

resistance of the target. The illustrated phenomenon explains how a large amount of resources have been wasted on the use of a prescribed equivalent horizontal force to represent an impact hazard when the self-weight of the target has not been factored into the design.

The analytical model of Eqs.(5a) – (5g) was employed for estimating the maximum deflection of the RC member for Large scale impact testing of RC beams conducted by Fujikake (2009). Results of the comparative study which are summarised in Fig. 8 in the form of bar charts present the maximum deflection value which was obtained by different means for the considered impact scenario. Results obtained from calculations which made use of closed-form expressions associated with the individual analytical models are first presented. Test results were then used as benchmarks for comparison with the calculated estimates (Fig. 8). It is shown that the DB model which is represented by Eqs. (5a) – (5g) achieves much better match with the test results than the other two analytical models that have been included in the comparative study, and is slightly more conservative than results obtained from LS DYNA simulations and from the experiments. Fig. 8 only presents a sample of the results.

Once the value of the maximum deflection (Δ) is known the bending moment at mid-span of a simply-supported beam can be found using Eq. (7) provided that the beam responds within the linear elastic limit.

$$M_{el} = \frac{12EI\Delta}{L^2} \tag{7}$$

Should the yield limit be surpassed Eq. (8) may be used to solve for plastic hinge rotation (φ_{pl}).

$$\varphi_{pl} = \frac{1}{1+\lambda}\frac{mv_0^2}{2M_{pl}} - \frac{M_{pl}L}{6EI} \tag{8}$$

where M_{pl} is moment developed at the plastic hinge

Eq. (8) may be derived by combining Eq.(5g) with elementary relationships of statics and kinematics of a simply-supported single span member experiencing plastic hinge rotation at the mid-span position.

5. SIMULATION OF DEBRIS HAZARD

An analytical model based on a two-degree-of-freedom (2DOF) spring mass model as illustrated in Fig. can be used to simulate the occurrence of contact force in the course of the impact. Whilst the analytical model is simple and computationally inexpensive to operate results so obtained have been found to be in excellent agreement with the measured results (Sun 2015b; Perera 2015). The analytical model introduced herein enables time-histories of both the contact force (and the indentation) to be simulated alongside the target deflection. Lumped mass m_1 and m_2 represent the impactor and its target whereas displacements and energy dissipation are emulated using springs (k_n, p and k_2) and dampers (D_n). Generalised mass m_2 and stiffness k_2 values of target structures are relatively easy to be determined (Yang 2012a & 2012b).

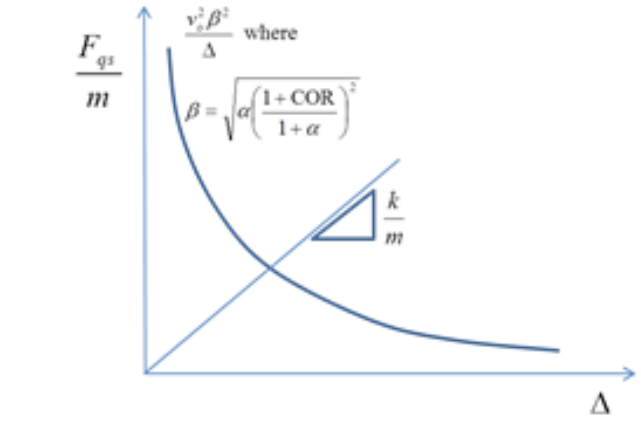

(a) ADRS diagram for impact action

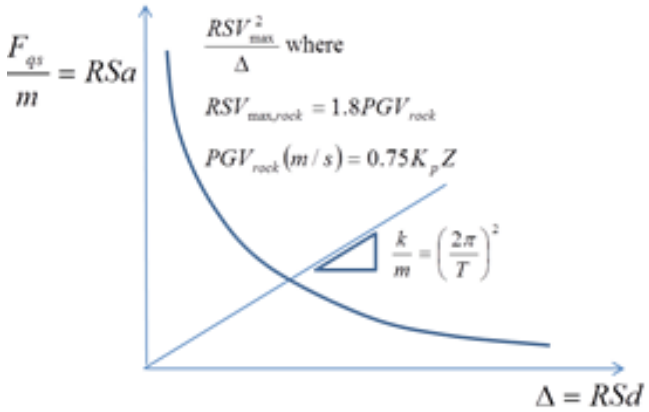

(b) ADRS diagram for seismic action

Fig. 6 Acceleration-Displacement Response Spectrum (ADRS) Diagrams

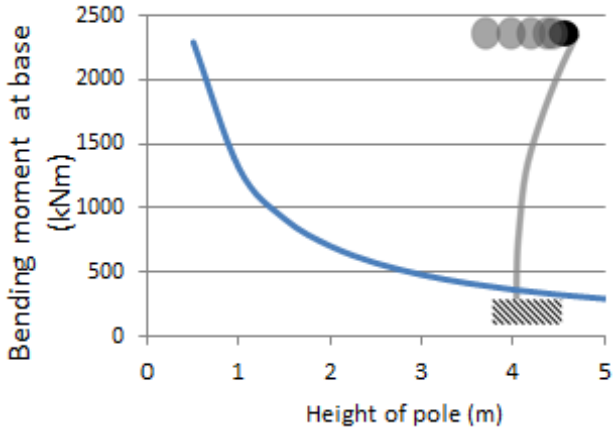

Fig. 7 Bending moment value at base of pole

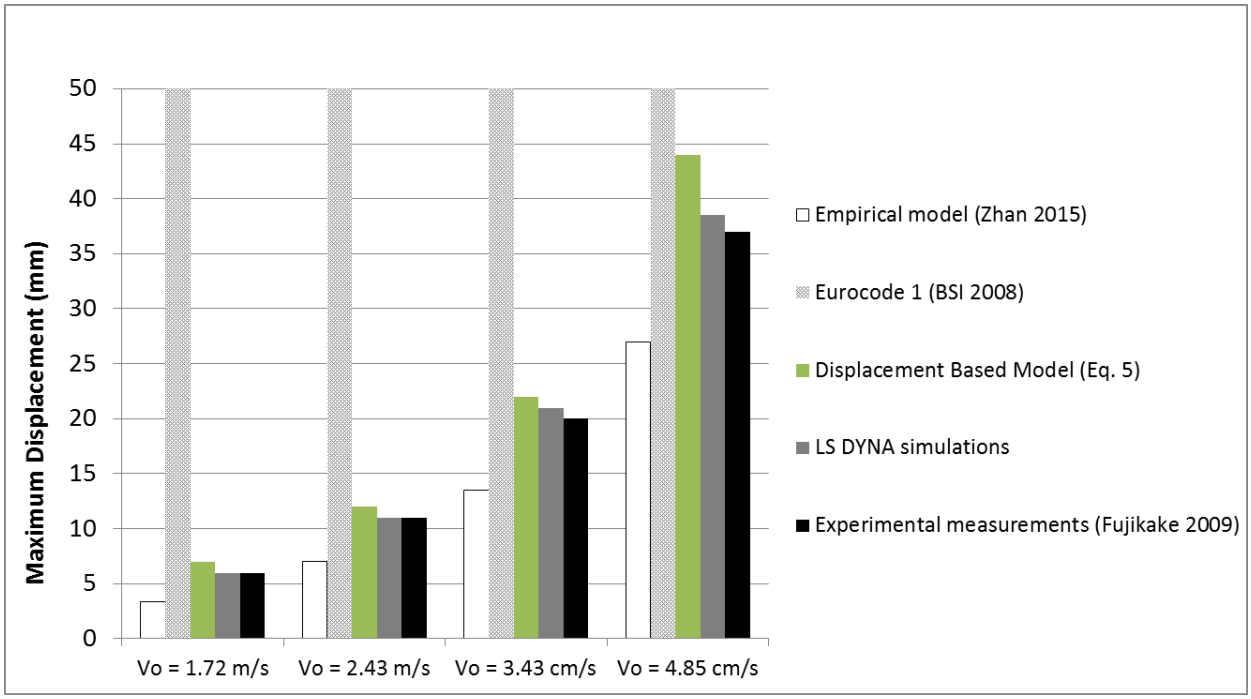

Fig. 8 Results from analytical models, LS DYNA simulations and experiments

The time-history of the contact force, $F_c(t)$, can be obtained by solving the following differential equation which is based on *non-linear viscous elastic* behaviour at contact (Hunt & Crossley 1975).

$$F_c(t) = D_n\delta^p(t)\dot{\delta}(t) + k_n\delta^p(t) \tag{9}$$

where $\delta(t)$ and $\dot{\delta}(t)$ are indentation and indentation velocity respectively.

The use of Eq. (9) for determining the forcing function at contact (i.e. function of contact force) requires the values of parameters k_n, p, and D_n to be known beforehand. However, values of the dynamic contact stiffness parameters (k_n, p, and D_n) which characterise the properties of the frontal spring in the 2DOF model have not been well documented, and more so for debris materials. Experimental impact test data derived from the impact testing for a range of debris materials including hailstones has been used to determine the values of parameters k_n, p, and D_n and its variation with the incident velocity of impact (Sun 2015b; Perera 2015). Once the parameter values are known (for a given impact velocity) the forcing function at contact generated by a range of impact scenarios can be modelled reliably by solving Eq. (9) based on the use of established numerical techniques. For example, numerical integration executable by elementary *row-and-column* operations on an EXCEL spreadsheet can be used for finding the forcing function (Sun 2016).

Consider a piece of concrete debris weighting 300 g, and 62.5 mm in size, impacting onto a square aluminium alloy plate of dimensions: 300 mm×300 mm×4 mm at an incident velocity of 24.5 m/s. Inputting values of parameters into an Excel spreadsheet for numerical integration leads to the solution of F_{cmax} = 20 kN (Fig. 10). Results are similarly obtained for impact velocities of 24.5 m/s, 36 m/s and 48 m/s and

for different debris materials.

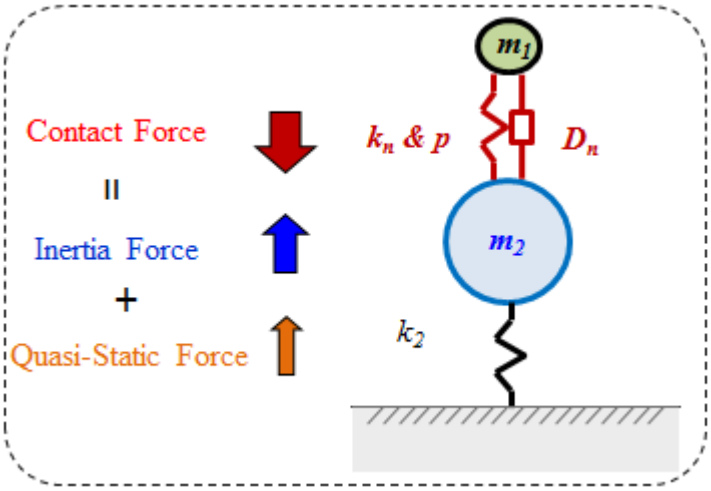

Fig. 9 2DOF spring connected lumped mass model

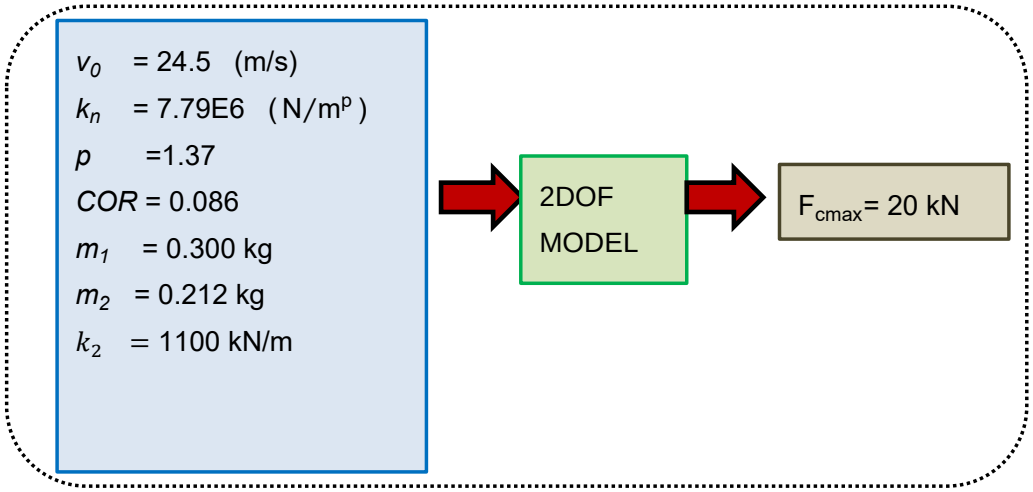

Fig. 10 Max. contact force generated by impact of concrete debris at 24.5 m/s

Impact parameters at velocity of 24.5 m/s is summarised as follows: v_0 = 24.5 m/s; m_1=0.3 kg; m_2 = 0.21 × total plate mass = 0.21 × 1.008 = 0.212 kg; k_2 = 1100kN/m; α = m_2/m_1 = 0.706; COR = 0.086. These parameter values when substituted into Eqs. (5a) – (5g) give estimates for the (equivalent) statically applied load to result in the deflection of the target matching with the deflection of impact. The calculation is shown in below.

$$\beta = \sqrt{\alpha\left[\frac{1+COR}{1+\alpha}\right]^2} = \sqrt{0.706\left[\frac{1+0.086}{1+0.706}\right]^2} = 0.535 \quad (10a)$$

$$\Delta = \beta\,\frac{m_1 v_0}{\sqrt{m_1 k_2}} = 0.535 \times \frac{0.3\times 24.5}{\sqrt{0.3\times 1100000}} = 6.9\ mm \quad (10b)$$

$$F = k_2\Delta = 1100000 \times 0.0069 = 7.5\ kN \quad (10c)$$

It is noted that the equivalent static force of 7.5 kN which is representative of the impulsive effects of the impact is much less than the predicted contact force value of 20 kN (as shown by Fig.10). Widespread denting to metal claddings and roof coverings by debris impact in extreme weather conditions could not possibly be the result of the impact generated impulsive actions (estimated by the use of energy and momentum principles). What caused the indentation, or perforation, in severe storm scenarios was the much higher contact force which was localised around the point of contact.

The forcing function at contact so derived from the analytical (2DOF) model has been applied quasi-statically on a common test rig for the damage assessment of the target specimen. The 300 mm×300 mm×4 mm aluminium plate specimen was tested on the MTS 250 kN Dynamic UTM Model 819 high rate testing machine. The rate of loading on the test rig was approximately consistent with the actual impact conditions for determining the *force-deflection* relationship and the perforation capacity of the aluminium plate. Load was applied onto the surface of the target plate through a 62.5 mm diameter steel ball bearing. The recorded load-deflection profiles of the target specimen from quasi-static testing at different loading rates are shown in Fig. 1 which shows that the target stiffness (gradient of load-deflection curve) increases steadily with increasing rate of loading.

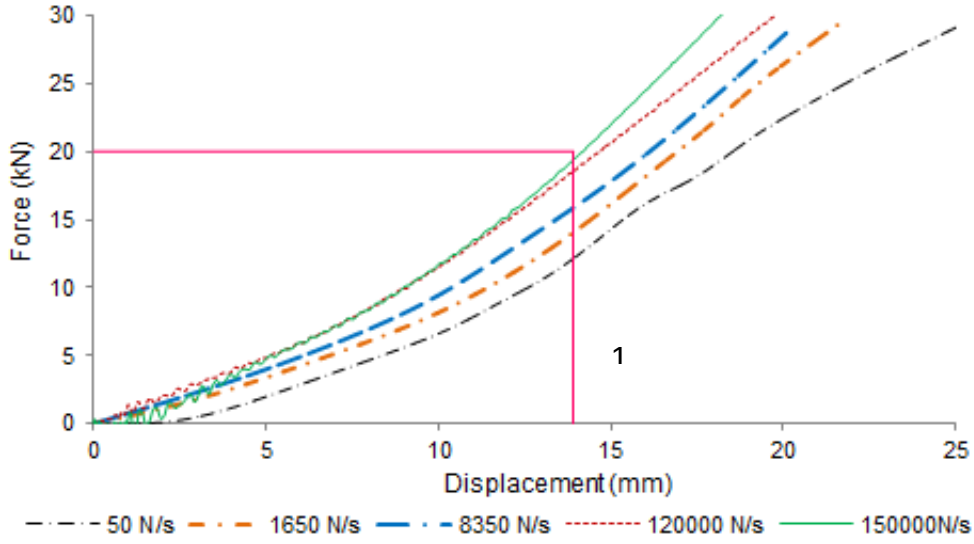

Fig. 11 Load-deflection relationship of 4 mm Aluminium plate

Results reported for the loading rate of 150 kN/s was the highest loading velocity that can be achieved through the MTS 250 kN machine. The stiffness of the target material was observed to be 1100 kN/m (at a loading rate of150 kN/s). Now, recall the impact of the concrete debris on the aluminium alloy plate at velocity of 24.5 m/s producing a contact force value of 20 kN and a maximum deflection of 13.9 mm (Fig. 10 & 11). The machine which was in the force-controlled mode and made to unload as soon as the targeted load limit of 20 kN was reached. The tested specimen was unbolted and its final deformation profile was measured using a 0.01 mm accuracy dial gauge.

Photo images taken from the two plate specimens that have been subject to the (a) quasi-static test and (b) impact test are shown in Fig. 12(a) and 12(b) respectively.

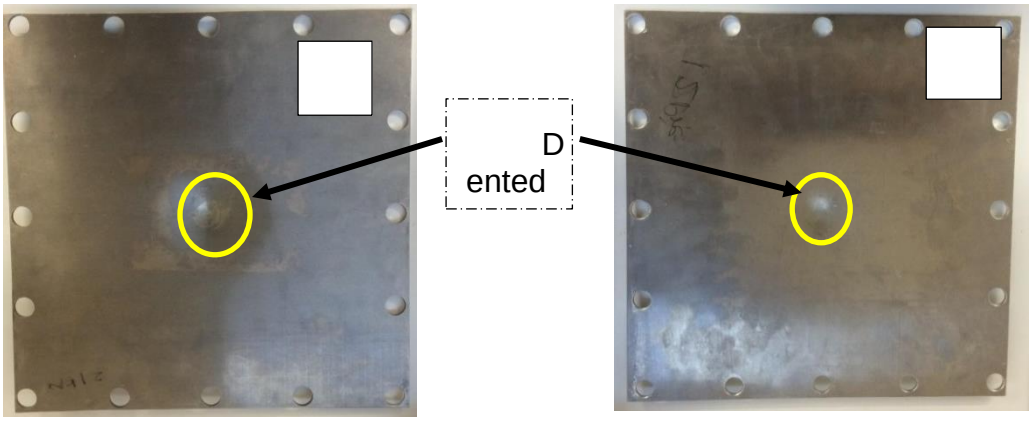

Fig. 12 (a) Quasi-statically tested plate; (b) impact tested plate

The target specimen has also been tested on the (250 kN capacity) high speed test machine at a rate of 150 kN/s (corresponding to 0.1 m/s approximately) up to the point of perforation of the plate. It is indicated from the load- deflection relationship obtained from the quasi-static experiment that a 13.9 mm deflection is predicted for a contact force value of 20 kN (Fig.13a). In comparison, the amount of deflection produced by accelerating the debris specimen directly onto the plate (in the impact experiment) was 12.5 mm (Fig. **1**3b). Discrepancies between the two results were minor and can be explained by reference to differences in the strain rates adopted in the two tests (noting that the rate of loading rate in the impact test was 1000 times higher than that in the quasi-static test).

The comparative study was aimed at demonstrating that applying the contact force on a static test-rig could be used to provide sufficiently accurate estimates of the nature and extent of the damage. The amount of deflection caused to the same alloy plate by the impact of a different debris material with different velocities of impact (e.g. 24.5 m/s, 36 m/s and 48 m/s) can also be found in the manner illustrated. For example, a piece of a 62.5 mm dia. hailstone is predicted to generate a contact force of 5.4 kN and deflect the alloy plate by 5.5 mm at v_0 = 24.5 m/s; the contact force value is increased to 10 kN and deflection increased to 9 mm at v_0 = 36 m/s. The quasi-static experiment was also able to provide information on the ultimate capacity of the target (plate) up to the point of causing perforation which occurred at 80 kN in comparison with the 20 kN generated by the impact (Fig. 13a).

In summary, a demand versus capacity comparison of this nature (indicating the margin of safety from perforation) would not have been possible with conventional impact testing in which case projectiles would need to be accelerated onto the target in a repetitive manner in increments of velocity to determine the ultimate impact resistant capacity of the cladding material.

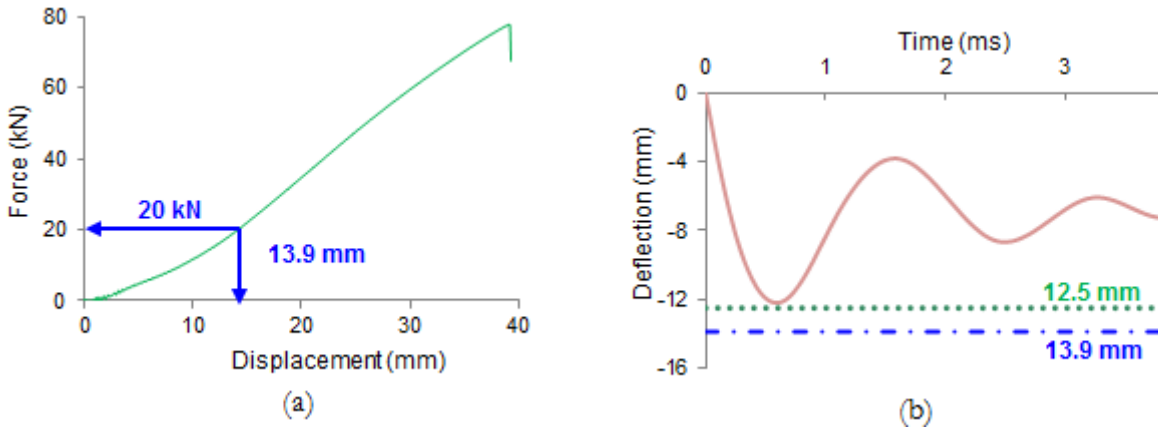

Fig. 13 (a) Load-deflection profile of 4 mm test plate up to perforation at loading rate of 1500 kN/s; (b) Deflection time-history measured from the impact test using the laser device

6. CLOSING REMARKS

A review of the state-of-the-art of the subject was first presented covering impact actions on RC members, vehicular barriers and building facades. A design procedure involving the use of some closed-form expressions along with a design chart for estimating the factor of safety against overturning of a rectangular barrier was then presented. More closed-form expressions were introduced for estimating the deflection demand of the impact on a RC member associated with the impulsive action. This method is also known as the Displacement Based (DB) Method of modelling impact actions. The accuracies of the DB method were then demonstrated by comparison with results from experimental measurements and numerical simulations using program LS-DYNA. The idea of solving for the impulsive action by the use of response spectra (presented in the conventional acceleration format and the ADRS format) in a manner similar to that used for solving for seismic actions was then presented. Finally, the use of numerical integration technique (which can be implemented on Excel) for the determination of the contact force was presented. It was demonstrated in a comparative study that applying the identified forcing function on a metal plate in a quasi-static manner would be able to simulate damage that was inflicted by acceleration an impactor object directly on the metal plate at a given velocity of impact.

7. ACKNOWLEDGEMENTS

Input from research collaborators and PhD candidates who contributed to the creation of materials that have been included in this review article is gratefully acknowledged. Financial support from the Australian Research Council (ARC) Discovery Project DP170101858 entitled *New Approach for Design of Barriers For Impact* is gratefully acknowledged. Specific acknowledgement goes to Arnold Yong and Carlos Lam for their contributions to materials presented in Sec. 3; Arnold Yong for Sec. 4 and Shihara Perera and Mahil Tharindu for Sec. 5.

8. REFERENCES

AEES (2009). Commentary to the AS1170.4: Structural design actions - part 4 earthquake actions. Australian Earthquake Engineering Society.

Ali M, Sun J, Lam N, Zhang L, Gad E. (2014) Simple hand calculation method for estimating deflection generated by the low velocity impact of a solid object. Australian Journal of Structural Engineering, 15(3), 243-259.

Alphonso, T.C. and M. Barbato (2014) Experimental fragility curves for aluminum storm panels subject to windborne debris impact. Journal of Wind Engineering and Industrial Aerodynamics, 134(0), 44-55

American Association of State Highway and Transportation Officials, AASHTO (2012) LRFD Bridge Design Specifications, 6th edition, Washington DC, U.S.

ASTRA (2008) Einwirkungen infolge Steinschlags auf Schutzgalerien (in German). Richtlinie, Bundesamt für Strassen, Baudirektion SBB, Eidgenössische Drucksachen-und Materialzentrale, Bern.

Austroads (2013) Standardised Bridge Barrier Design. 2013, Sydney: Austroads Ltd.

Berthet-Rambaud, P., Timsah, Y., Daudeville, L., and Mazars, J.(2003) Finite element modelling of concrete protection structures submitted to rock impacts. in 16th ASCE Engineering Mechanics Conference, University of Washington, Seattle.

British Standard Institute, BSI (2008) Eurocode 1 - Actions on structures - Part 1-7: General actions - accidental actions (S.P. Committee, Ed.), European Committee for Standardization, London.

Chen, Y. and May, I.M. (2009), Reinforced concrete members under drop-weight impacts. Proceedings of the ICE - Structures and Buildings, 162(1), 45-56.

Chen, W., H. Hao, and H. Du (2014) Failure analysis of corrugated panel subjected to windborne debris impacts. Engineering Failure Analysis, 44(0), 229-249.

Chen, W. and H. Hao (2015) Performance of structural insulated panels with rigid skins subjected to windborne debris impacts – Experimental investigations. Construction and Building Materials, 77(0), 241-252.

Chikatamarla, R., Laue, J., and Springman, S. (2004) Rockfall impact on protection galleries. in Second International Conference of Structural Engineering Mechanics and Computations, Balkema, Rotterdam, Cape Town, South Africa, 1139-1144.

Delhomme, F., Mommessin, M., Mougin, J., and Perrotin, P.(2007), Simulation of a block impacting a reinforced concrete slab with a finite element model and a mass-spring system. Engineering Structures, 29(11), 2844-2852.

Fernandez, G., Masters, F.J. and Gurley, K.R. (2010) Performance of hurricane shutters under impact by roof tiles. Engineering Structures, 32(10), 3384-3393..

Frye, U., Ginger, J. and Leitch, C. (2012) CTS. Cyclone testing-response of metal cladding systems to windborne debris impact (technical report 59). Cyclone Testing Station, James Cook University.

Fujikake, K., Li, B., and Soeun, S. (2009) Impact Response of Reinforced Concrete Beam and Its Analytical Evaluation. Journal of Structural Engineering, 135(8), 938-950.

Goyal, V.K., C.A. Huertas, and T.J. Vasko (2013) Smooth Particle Hydrodynamics for Bird-Strike Analysis Using LS-DYNA.

Herbin, A. and M. Barbato (2012) Fragility curves for building envelope components subject to

windborne debris impact. Journal of Wind Engineering and Industrial Aerodynamics, 107, 285-298.

Hummeltenberg, A., Beckmann, B., Weber, T., and Curbach, M. (2011) Investigation of concrete slabs under impact load. Applied Mechanics and Materials, 82, 398-403.

Hunt, K.H. and Crossley, F.R.E. (1975) Coefficient of Restitution Interpreted as Damping in Vibroimpact. Journal of Applied Mechanics, 42(2), 440.

Japan Road Association, JRA (2000). "Manual for Anti-impact Structures against Falling Rock (in Japanese)."

Kishi, N. and Bhatti, A.Q. (2010) An equivalent fracture energy concept for nonlinear dynamic response analysis of prototype RC girders subjected to falling-weight impact loading. International Journal of Impact Engineering, 37(1), 103-113.

Kishi, N. and Mikami, H. (2012) Empirical Formulas for Designing Reinforced Concrete Beams under Impact Loading. ACI Structural Journal, 109(4), 509-519.

Kishi, N., Okada, S.-Y., and Kon-No, H.(2009) Numerical impact response analysis of rockfall protection galleries. Structural Engineering International, 19(3), 313-320.

Lam, N.T.K., Yong, A.C.Y., Lam, C., Kwan, J.S.H., Perera, J.S., Disfani, M. and Gad, E.F. (2017) Novel Displacement-Based Approach for the Assessment of Overturning Stability of Rectangular Rigid Barriers Subjected to Impact, ASCE Journal of Engineering Mechanics (in press)

LS-DYNA, Keyword user's manual. 2015: Livermore Software Technology Corporation (LSTC).

Mougin, J. P., Perrotin, M., Mommessin, J. Tonnelo and Agbossou , A. (2005). "Rock fall impact on reinforced concrete slab: an experimental approach." International journal of impact engineering, 31(2), 169-183.

Perera, S., Lam, N., Pathirana, M., Zhang, L., Ruan, D., and Gad, E,(2016) Deterministic solutions for contact force generated by impact of windborne debris. International Journal of Impact Engineering,. 91, 126-141.

Raguraman, M., et al. (2008) Numerical Simulation of Projectile Impact on Mild Steel Armour Platesusing LS-DYNA, Part II: Parametric Studies. Defence Science Journal, 58(4), 573.

Standards Australia (2004). AS5100.2 Bridge Design Part 2: Design Loads. New South Wales, Australia.

Sun, J., Lam, N., Zhang, L., Gad, E., and Ruan, D.(2015a) Contact forces generated by fallen debris. Structural Engineering and Mechanics, 50(5), 589-603.

Sun, J., Lam, N., Zhang, L., Ruan, D., and Gad, E.(2016) Computer Simulation of Contact Forces Generated by Impact. International Journal of Structural Stability and Dynamics, DOI: 10.1142/S0219455417500055.

Sun, J., Lam, N., Zhang, L., Ruan, D., and Gad, E.(2015b) Contact forces generated by hailstone impact. International Journal of Impact Engineering, 84, 145-158.

Thai, D.-K. and Kim, S.-E.(2014) Failure analysis of reinforced concrete walls under impact loading using the finite element approach. Engineering Failure Analysis, 45, 252-277.

Wu, M., Chen, Z., and Zhang, C. (2015) Determining the impact behavior of concrete beams through experimental testing and meso-scale simulation: I. Drop-weight tests. Engineering Fracture Mechanics, 135, 94-112.

Wu, Y., Crawford, J.E., and Magallanes, J.M. (2012) Performance of LS-DYNA concrete constitutive models. in 12th International LS-DYNA Users Conference.

Yahya, M.F., et al. (2012) Finite element analysis of impactor shapes effects on puncture damage of plain woven fabric. in Humanities, Science and Engineering (CHUSER), IEEE Colloquium.

Yang Y, Lam N, Zhang L. (2012a) Evaluation of simplified methods of estimating beam responses to impact. International Journal of Structural Stability and Dynamics,12(03).

Yang Y, Lam N, Zhang L. (2012b) Estimation of Response of Plate Structure Subject to Low Velocity Impact by a Solid Object. International Journal of Structural Stability and Dynamics,12(6)-art no. 1250053.

Zhan, T., Wang, Z., and Ning, J. (2015) Failure behaviors of reinforced concrete beams subjected to high impact loading. Engineering Failure Analysis.

Tsang, H.H. and Lam, N.T.K. (2017) Earthquake Loading Characterisation for Regions of Low to Moderate Seismicity, procs. of ANBRE17 symposium, Seoul, Korea. Paper ID: ES2373_3450.

Zhou, H., K. Dhiradhamvit, and T.L. Attard (2014) Tornado-borne debris impact performance of an innovative storm safe room system protected by a carbon fiber reinforced hybrid polymeric-matrix composite. Engineering Structures, 59(0), 308-319.

Zineddin, M. and Krauthammer, T. (2007) Dynamic response and behavior of reinforced concrete slabs under impact loading. International Journal of Impact Engineering, 34(9), 1517-1534.